15th International Conference on Combustion Technologies for a Clean Environment
June 25-29, 2023, Lisbon, Portugal

Analysis of the Performance of Kinetic Reaction Mechanisms in Estimating N_2O Mole Fractions in 70/30 vol% NH_3/H_2 Premixed Flames

Alnasif A[a,b*], Jójka J[c], Mashruk S[a], Nagy T[d], Valera-Medina A[a]

[a] College of Physical Sciences and Engineering, Cardiff University, Queen's Building, Cardiff CF24 3AA, United Kingdom
[b] Engineering Technical College of Al-Najaf, Al-Furat Al-Awsat Technical University, Najaf, 31001, Iraq
[c] Institute of Thermal Engineering, Poznan University of Technology, 60-965 Poznan, Poland
[d] Institute of Materials and Environmental Chemistry, Research Centre for Natural Sciences, 1117 Budapest, Hungary

ABSTRACT

To decrease the negative impact of fossil fuels, it is important to search for an alternative to decarbonize fuel sources. Ammonia (NH_3) is an attractive fuel candidate to reduce the CO_2 emission and hydrocarbon pollutants. NH_3 has many advantages that include its production from renewable sources, whilst enjoying a large storage and transportation network with comparable combustion properties to coals and alcohols. However, NH_3 has drawbacks represented by high NOx emissions which can considerably increase when NH_3 is blended with H_2. It is important to study the chemistry of NH_3 whilst investigating the NOx kinetic mechanisms to be aware of the causative parameters behind this matter. The present study deals with analysing the performance of various kinetic reaction mechanisms from the literature in terms of estimation of N_2O mole fraction. Sixty-eight chemical kinetic mechanisms have been analysed numerically by Chemkin-Pro software. A preliminary estimation has been conducted applying a symmetric mean absolute percentage error (SMAPE) to compare the numerical outcomes with the experimental measurements from the literature to highlight the kinetic models with low level of discrepancy and proper estimation of N_2O mole fractions. The sensitivity analysis along with rate of production/consumption of N_2O investigation at several conditions of equivalence ratio (0.6,1,1.4) has been conducted to check the discrepancies among the mechanisms and shed light on the reactions that dominate the formation/consumption of N_2O at different conditions. The study found that the kinetic model developed by Klippenstein et al. (2018) accurately predicts N_2O mole fraction. However, the model's precision decreases as the equivalence ratio increases from 1 to 1.4. Along with that the rate of production/consumption analysis revealed the NH+NO=N_2O+H reaction has a dominant role in the formation of N_2O for all studied conditions, while the consumption of N_2O is dominated by reactions N_2O+H=N_2+OH, N_2O (+M) =N_2+O(+M) and N_2O+NH_2=N_2H_2+NO at all analysed conditions.

Keywords: Kinetic reaction mechanism, Ammonia, Burner stabilised-stagnation flow, Kinetic modelling N_2O mole fraction.

1. INTRODUCTION

The vast spreading population and rapid economic development in recent decades have affected dramatically the global energy consumption. Fossil fuel sources such as coal, petroleum and natural gas are kept at the top of the major energy sources across the world. The emissions and the pollutants that can be released by the combustion of these fossil fuels include CO_2, CO, NOx, SO_2, volatile compounds, particulate matter, etc. which have extremely negative impacts on the ecosystem [1]. Due to the negative effects of CO_2, it has been necessary to develop new technologies that aim to reduce problems that correlate with energy consumption. These factors combined with more strict regulations lead to investigate carbon-free fuel sources linked to renewable energy resources [2]. Ammonia (NH_3) is a promising alternative carbonless fuel due its high hydrogen density content, hence making it an attractive hydrogen carrier fuel. The fuel enables 1) CO_2, SOx and soot emission free flue gases; 2) producibility from different sources such as renewable sources and biomass; 3) transportation and storage can be done using working existing infrastructure. All these factors make NH_3 a favourably clean fuel candidate for the energy sector. However, high NOx emission and narrow flammability

*Corresponding author email: AlnasifAH@cardiff.ac.uk

limits are the main problem that restricts the use of NH_3 in large-scale thermal devices [3,4]. The combustion properties of NH_3, in terms of laminar burning velocity, have been studied and improved by blending NH_3 with other doping agents as a fuel. However, this can increase NOx emissions [3–6].

The term NOx stands for all nitrogen oxide forms generated by combustion, which are mainly nitric oxide (NO), nitrogen dioxide (NO_2) and nitrous oxide (N_2O). The greenhouse effect of N_2O is also very important as it has 300 times larger Global Warming Potential than CO_2 [7,8]. Several experimental and numerical studies have been carried out on NH_3-H_2 blends in terms of N_2O emission [9–11]. It has been found that the concentration of N_2O reaches its peak at 85/15 vol% NH_3/H_2 with a thermal power of 20kW and a Reynolds number of 40,000.[9]. Numerically, many studies have been carried out on NH_3 in terms of understanding the chemical kinetics of NH_3 combustion to improve the reaction mechanism of NOx. The performance of most advanced kinetic models was improved on the basis of experiments conducted on many combustion configurations, an exercise that resulted in adding new reactions or updating Arrhenius parameters that govern the rate of reactions [12–15].

The current study aims to analyze the performance of kinetic reaction mechanisms for estimating N_2O in a 70/30 vol% NH_3/H_2 blended fuel at the full range of equivalence ratios (0.6-1.4). Additionally, the study aims to identify the reaction steps responsible for N_2O formation/consumption and reveal the reasons for discrepancies in the estimation of experimental measurements of N_2O in ammonia combustion systems.

2. NUMERICAL SETUP AND KINETIC MODELING

Chemkin-Pro package of ANSYS software was used to study the performance of 68 chemical kinetic mechanisms in stabilised-stagnation flame simulations. The numerical simulations applied the same boundary conditions as those used in the experiments in terms of atmospheric conditions, plate temperature and inlet velocity of the blend, Table 1. Also, the length of the computational domain was set to 2 cm in accordance with the distance of the top plate from the nozzle burner used in the experiments. In addition, the maximum number of grid points allowed with adaptive grid control, gradient and curvature thresholds were set to 5000, 0.01, 0.01, respectively.

Table 1. Boundary conditions used in the experiments

#	Equivalence ratio φ	V_{in} (cm/s)	Plate temperature T_W (K)
1	0.6	25.53	493.5
2	0.8	31.26	511.5
3	1.0	42.57	563.6
4	1.2	40.96	574.7
5	1.4	30.86	504.0

Table 2 lists the tested kinetic reaction mechanisms in this present study in terms of the number of species and reactions. The experimental measurements have been conducted at Tohoku University using a stagnation flame configuration to determine the concentration of N_2O from the combustion of 70/30 vol% NH_3/H_2 blended fuel. The details of the experimental setup can be found elsewhere

Table 2: Kinetic reaction mechanisms adopted in the present study.

#	Kinetic mechanism	No. of reactions	No. of species	Ref.	#	Kinetic mechanism	No. of reactions	No. of species	Ref.
1	Bertolino et al., 2021	264	38	[16]	35	Dagaut et al., 2008	250	41	[17]
2	Mei, Ma, et al., 2021	264	38	[18]	36	Gregory et al., 2000	325	53	[19]
3	Han et al., 2021	298	36	[20]	37	Coda Zabetta & Hupa, 2008	371	60	[21]
4	Mei, Zhang, et al., 2021	257	40	[22]	38	Alzueta MU, 2016	654	131	[23]
5	Gotama et al., 2022	119	26	[12]	39	Shmakov et al., 2010	1207	127	[24]
6	Shrestha et al., 2021	1099	125	[25]	40	Esarte et al., 2011	536	79	[26]
7	Z. Wang et al., 2021	444	91	[27]	41	Abian et al., 2015	201	31	[28]
8	X. Zhang et al., 2021	263	38	[29]	42	T. Wang et al., 2018	925	81	[30]
9	Arunthanayothin et al., 2021	2444	157	[31]	43	T. Faravelli, 2017	158	29	[32]
10	Stagni et al., 2020	203	31	[15]	44	POLIMI, 2014	155	29	[33]
11	Han et al., 2019	177	35	[34]	45	Marques et al., 2073	318	61	[35]
12	De Persis et al., 2020	647	103	[36]	46	Aranda et al., 2013	566	95	[37]
13	Mei et al., 2019	265	38	[38]	47	Jiang et al., 2020	60	19	[39]
14	Li et al., 2019	957	128	[40]	48	Sun et al., 2022	486	66	[41]
15	Okafor et al., 2019	356	59	[42]	49	Song et al., 2019	158	29	[43]
16	Glarborg et al., 2018	231	39	[44]	50	Mével et al., 2009	203	32	[45]
17	Shrestha et al., 2018	1081	124	[46]	51	Da Rocha-Mathiue et al., 2019	66	22	[47]
18	Otomo et al., 2018	213	32	[48]	52	Da Rocha-Otomoet al., 2019	51	21	[47]
19	U. Mechanism, 2018	41	20	[49]	53	Da Rocha-Okafor et al., 2019	70	24	[47]
20	Klippenstein et al., 2018	211	33	[50]	54	Kovaleva et al., 2022	354	59	[51]
21	Nakamura et al., 2017	232	33	[13]	55	Houshfar et al., 2012 -Mid temp	91	26	[52]
22	Y. Zhang et al., 2017	251	44	[53]	56	Houshfar., 2012 -High temp et al	430	52	[52]
23	Lamoureux et al., 2016	934	123	[54]	57	Houshfar et al., 2012-Low temp	198	35	[52]
24	Xiao et al., 2017	276	55	[55]	58	Capriolo et al., 2021	2300	201	[56]
25	Song et al., 2016	204	32	[57]	59	Xu et al., 2023	389	69	[58]
26	Nozari & Karabeyoğlu, 2015	91	21	[59]	60	Thomas et al., 2022	1099	125	[60]
27	Mathieu & Petersen, 2015	278	54	[61]	61	Kovács et al., 2020a	214	34	[62]
28	Duynslaegher et al., 2012	80	19	[63]	62	Kovács et al., 2021	537	70	[64]
29	Klippenstein et al., 2011	202	31	[65]	63	Kovács et al., 2020b	214	34	[66]
30	K. Zhang et al., 2011	701	88	[67]	64	Saxena & Williams, 2007	288	59	[68]
31	Lamoureux et al., 2010	883	119	[69]	65	Valkó et al., 2022	537	70	[70]
32	Konnov, 2009	1207	127	[71]	66	Alzueta et al., 2001	464	65	[72]
33	Mendiara & Glarborg, 2009	779	79	[73]	67	Nakamura & Shindo, 2019	485	66	[74]
34	Tian et al., 2009	703	84	[75]	68	Glarborg, 2022	270	41	[14]

[76]. To examine the effect of equivalence ratio on the N_2O mole fractions, various equivalence ratios have been applied in the range of 0.6-1.4. A top stagnation plate was fixed 2 cm above the outlet section of the burner to manage generating a stagnation flow. The values of the top plate surface temperature and (T_W) and the mixture inlet velocity (V_{in}) were varied because of the variation in equivalence ratios and this variation changed the laminar burning velocity. The experimental data from [76] have been selected as it matched the conditions of our interest in terms of NH_3/H_2 ratio, the range of the equivalence ratio and the standard conditions of the unburned gas.

A symmetric mean absolute percentage error (SMAPE or sMAPE) formula has been adopted according to [77] to select the best kinetic reaction mechanisms that give better performance in the prediction of N_2O mole fraction when compared with the experimental data from [76].

$$SMAPE = \frac{|F_t - A_t|}{(A_t + F_t)} * 100\% \quad (1)$$

Where F_t: is the forecast from numerical calculations; and A_t: is the actual value from experiments.

3. RESULTS AND DISCUSSION

This section presents the results of the sensitivity analysis and the rate of production/consumption analysis of the most important reactions which affect N_2O. Fig. 1 shows the performance of the mechanisms by comparing their simulation results with the experimental measurements from [76] in terms of symmetric mean absolute percentage error (SMAPE). As a preliminary step, these error values were used to identify the reaction mechanisms that show low discrepancy with the experiments. While Fig. 2 shows the variation of mole fraction of N_2O as a function of equivalence ratio in the (0.6-1.4) range. The mole fraction of N_2O was taken at the end of the computational domain (at X=2cm), which corresponds to the sampling point of the experimental emission defined under steady state conditions. Because of the different trends at different equivalence ratios, the analysis will be presented for three categories, namely lean (φ=0.6), stoichiometry (φ=1) and rich flames (φ=1.4).

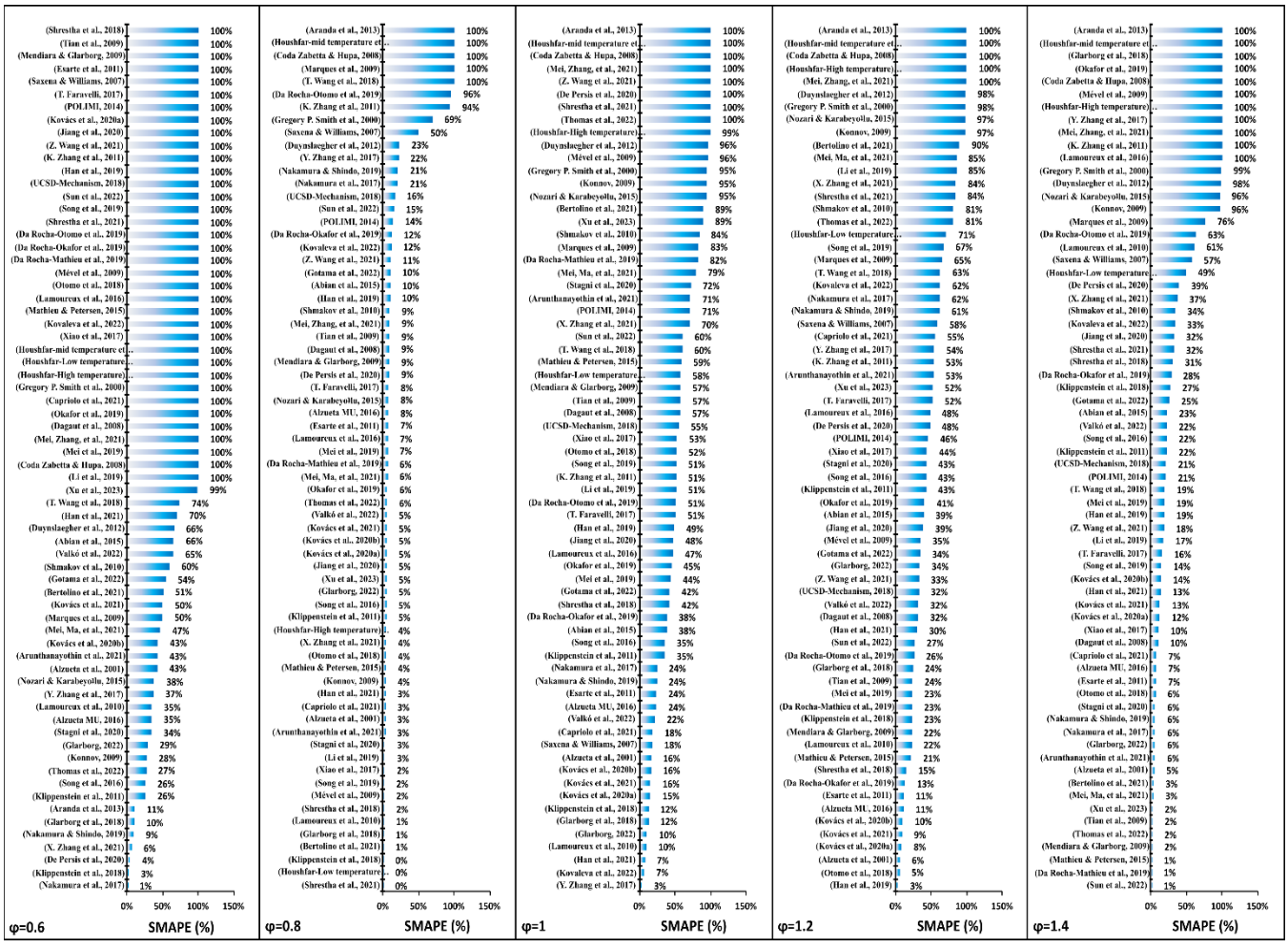

Fig. 1. Symmetric mean absolute percentage error (SMAPE) of N_2O mole fractions calculated by 68 reaction mechanisms at various equivalence ratios.

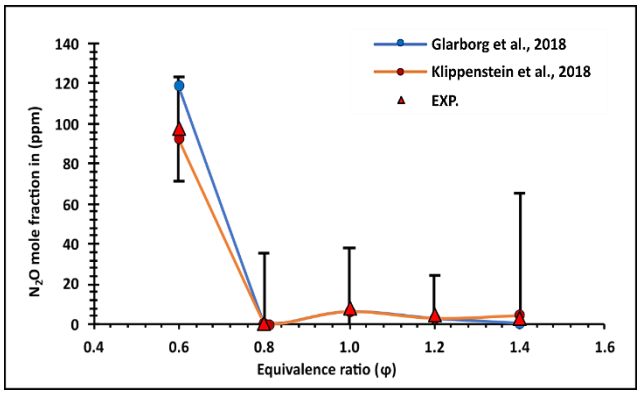

Fig.2. Variation of N2O concentration as a function of equivalence ratio.

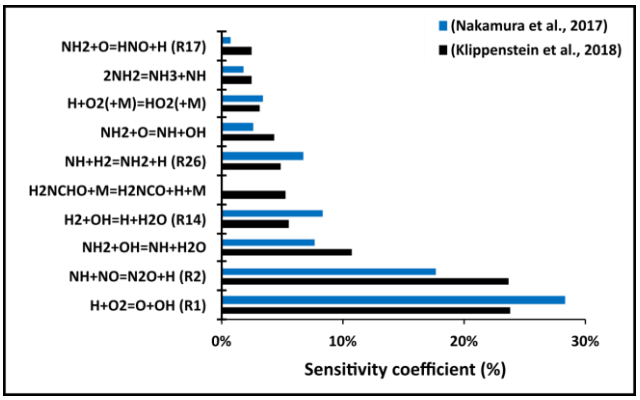

Fig.3. Reactions with the largest positive sensitivity coefficients for N_2O mole fractions in 70/30 vol.% NH_3/H_2 premixed flame at φ=0.6 in the Klippenstein and Nakamura kinetic models

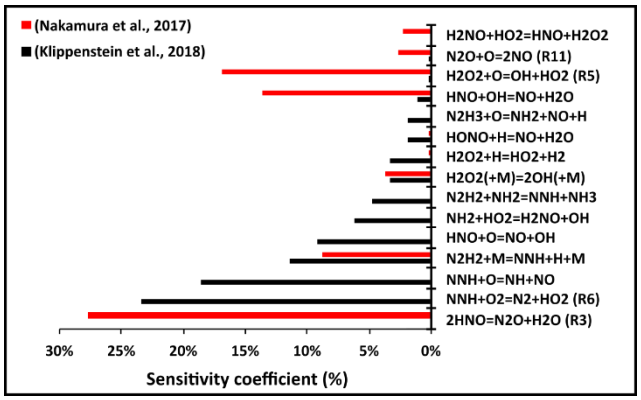

Fig.4. Reactions with the largest negative sensitivity coefficients for N_2O mole fractions in 70/30 vol.% NH_3/H_2 premixed flame at φ=0.6 in the Klippenstein and Nakamura kinetic models

3.1 Lean flame conditions

As can be seen from Fig. 2, the mole fraction of N_2O has its maximum value at φ=0.6, then it decreases sharply to zero as φ is increased to 0.8. Reaction mechanisms of (Glarborg et al, 2018) [44] and (Klippenstein et al, 2018) [50] show a good estimation for N_2O mole fraction when their outcomes compared with the experimental measurements along the lean range of 70/30 vol% NH_3/H_2 blended fuel. According to Fig. 1, the (Nakamura et al, 2017) kinetic model [13] shows 1% estimation error for N_2O mole fractions at φ=0.6, whilst Klippenstein's mechanism demonstrates better performance than the Glarborg's model. Therefore, both kinetic models, i.e., Nakamura and Klippenstein, will be investigated in detail with local sensitivity and rate of production/consumption analysis of N_2O to reveal the reasons behind the discrepancy among the selected mechanisms.

Figures 3 and 4 show the reactions with the largest positive and the negative sensitivity coefficients for N_2O mole fraction in the Nakamura and the Klippenstein mechanisms. The positive and negative sensitivity coefficients are normalized to their sum separately and shown as a percentage. As can be noticed from Fig. 3, reactions $H+O_2=O+OH$ (**R1**) and $NH+NO=N_2O+H$ (**R2**) are the most important for increasing N_2O mole fractions, furthermore, they are also promoting the system's reactivity via reactive H, O and OH radical formation. In addition to that, both selected kinetic models show different trends in sensitivity coefficients, which can be explained by the mechanistic differences and variations in the Arrhenius parameters which latter govern the rate of these reactions, which in turn determine the reactivity of the system, (see, Table 3).

In Figure 4, reactions $2HNO=N_2O+H_2O$ (**R3**), $HNO+OH=NO+H_2O$ (**R4**), and $H_2O_2+O=OH+HO_2$ (**R5**) show large negative sensitivity coefficients in Nakamura's kinetic model, indicating that they are the most important reactions responsible for decreasing the system reactivity and lowering the N_2O mole fractions, while Klippenstein's model identifies reactions $NNH+O_2=N_2+HO_2$ (**R6**) and $NNH+O=NH+NO$ (**R7**) as the most inhibiting ones for N_2O production. It can be noticed that reaction R3 has no impact on N_2O production in the Klippenstein model, whereas it appears to have substantial retarding effect in the Nakamura model.

Figures 5 and 6 show the variation of N_2O production and consumption rates as a function of distance, respectively, by the most important N_2O reactions in the Nakamura and the Klippenstein mechanisms.

As can be noticed from Figs. 5 and 6, the net production rate of N_2O increases when the temperature of the system increases sharply and then this is followed by a sudden decrease downstream. According to Nakamura's kinetic model, the climbing influence of the total component of N_2O is governed by the action of reaction R2 which is responsible for 99% of the N_2O formation in the combustion zone (see Fig. 7), while the decrease in N_2O is basically due to the retarding influence of reaction $N_2O+H=N_2+OH$ (**R8**) which accounts for 85% of the summed reaction rate of all N_2O consuming reactions (see Fig. 8). Similarly, Klippenstein's kinetic model shows an increase in the total N_2O due to the R2 reaction and then consumed by reactions R8 and $N_2O(+M)=N_2+O(+M)$ (**R9**), which thus are considered substantial in the consumption of N_2O (see Fig. 8).

The chemical pathways presented in Fig. 9 also show the dominant role of reaction R2 in the formation of N_2O, which indicates the dominant role of NH radicals in the production of N_2O (i.e. accounts for almost 98%), as well

as the substantial part of reaction R8 in the consumption of N_2O, which leads to production of N_2 and OH.

Figure 8 shows different trends among the selected mechanisms, where the Nakamura kinetic model shows higher level of N_2O consumption by reaction R8 compared to the Klippenstein model. Meanwhile, the rate of consumption of reactions R9, $N_2O+O=N_2+O_2$ (**R10**), $N_2O+O=2NO$ (**R11**) and $N_2H_2+NO=N_2O+NH_2$ (**R12**) in the Klippenstein kinetic model demonstrate higher values than those of the Nakamura model; what's more reaction R12 has negligible effect in the Nakamura mechanism. This differences in sensitivities can be justified by the variation of Arrhenius parameters that govern the reactions in each mechanism (see table 3), which affect the rate of the selected reaction (see Fig. 10). As noticed from Fig. 10 the Heat Release Rate (HRR) predicted by Klippenstein is greater than that estimated by Nakamura's model.

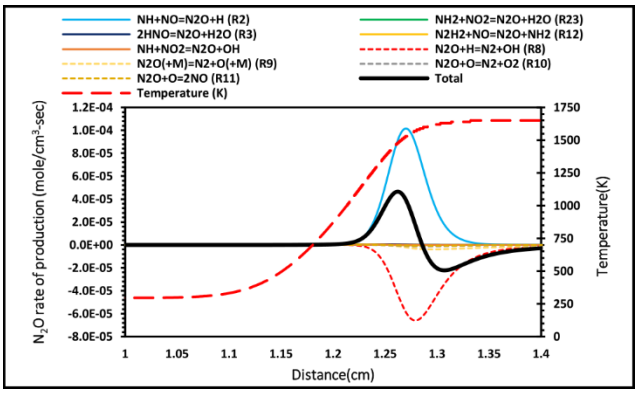

Fig.5. The rate of production/consumption of N_2O for 70/30 vol% NH_3/H_2 mixture at lean conditions estimated by model (Nakamura et al., 2017).

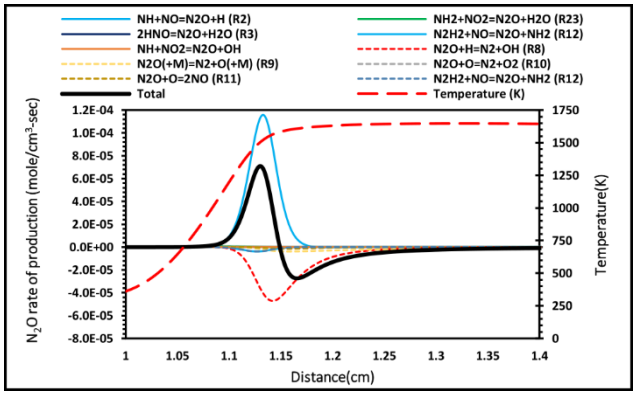

Fig. 6. The rate of production/consumption of N_2O for 70/30 vol% NH_3/H_2 mixture at lean conditions estimated by model (Klippenstein et al., 2018).

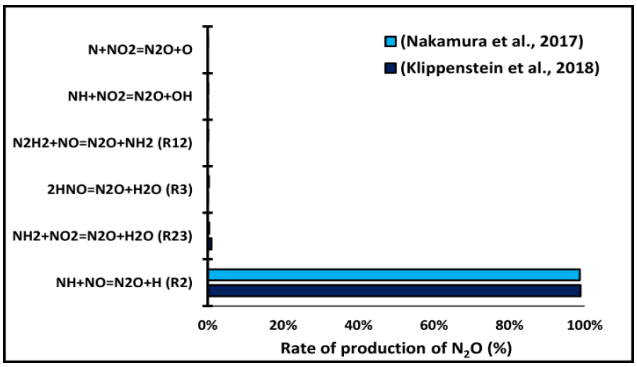

Fig. 7. Rate of production in (in %) at φ=0.6 estimated by the (Nakamura et al., 2017) and (Klippenstein et al., 2018) kinetic models.

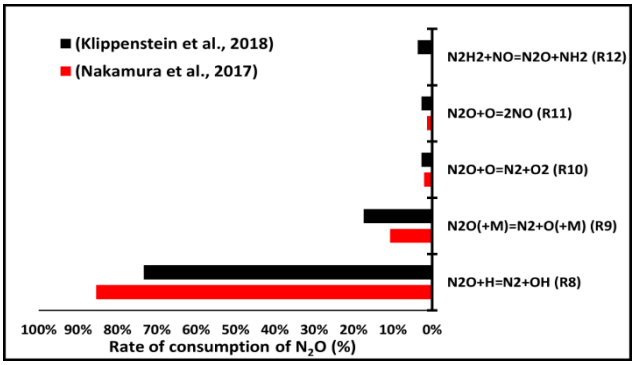

Fig. 8. Rate of consumption (in %) at φ=0.6 estimated by the (Nakamura et al., 2017) and (Klippenstein et al., 2018) kinetic models.

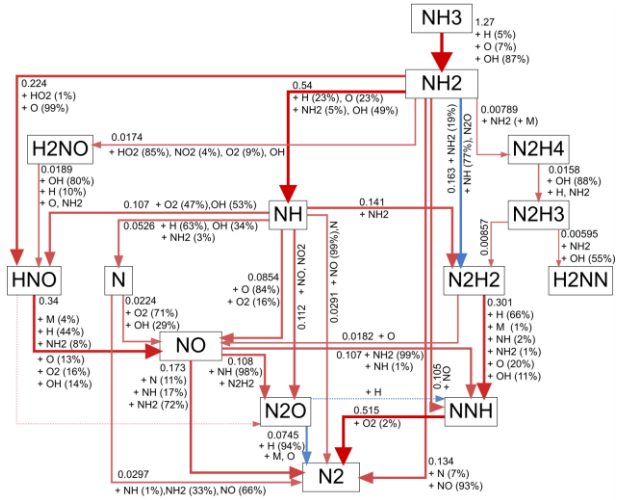

Fig. 9. Chemical reaction pathways of N_2O formation/consumption at flame zone (T= 1498 K) and at φ=0.6 predicted by the Klippenstein model. Arrow lines refer to chemical transformations, percentages (%) show to the contribution of a reactant to the transformation, numbers stand for the net reaction rate in kmol/m^{3}s, which is also visualized by line thickness.

Table 3: Key reactions of N_2O formation generated from Nakamura and Klippenstein kinetic models.

NO.	Reaction	(Klippenstein et al., 2018)			(Nakamura et al., 2017)		
		A	*n*	*E*	*A*	*n*	*E*
1	$H+O_2=O+OH$	1.00E+14	0.00	15286	1.040E+14	0.00	15286
2	$NH+NO=N_2O+H$	2.700E+15	-0.780	20	1.800E+14	-0.3510	-244.0
3	$N_2O+H=N_2+OH$	6.4E07	1.835	13492	3.310E+10	0.0000	5090.0
4	$N_2O(+M)=N_2+O(+M)$	9.9E10	0.000	57901	9.900E+10	0.0000	57960
5	$N_2O+O=N_2+O_2$	9.2E13	0.000	27679	3.690E+12	0.0000	15944.0
6	$N_2O+O=2NO$	9.2E13	0.000	27679	9.150E+13	0.0000	27693
7	$N_2H_2+NO=N_2O+NH_2$	4.0E12	0.000	11922	3.000E+10	0.0000	0.00

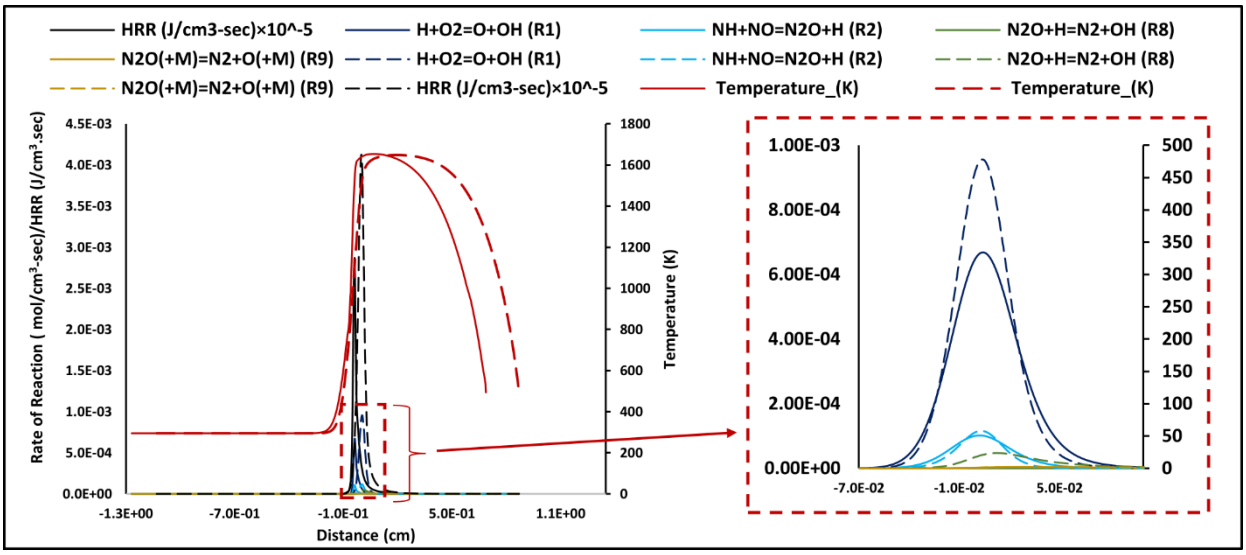

Fig. 10. The reaction rate profiles of reactions most influential to the formation/reduction of N_2O mole fractions for 70/30 vol% NH_3/H_2 mixture at φ= 0.6. The result for the (Nakamura et al., 2017) and (Klippenstein et al., 2018) models are shown with solid and dashed lines, respectively.

3.2 Stoichiometric flame conditions

Based on Fig. 2, it has been noticed that the mole fraction of N_2O is increased slightly. It has been shown that most of the tested mechanisms cannot prediction of N_2O mole fraction (see Fig. 1). The estimation accuracy of Klippenstein kinetic model has fallen back and the SMAPE increased to 12%. As can be seen from Fig. 1, the (Y. Zhang et al, 2017) kinetic model [53] shows low discrepancy levels ~3% compared to experimental measurements. Therefore, the Klippenstein and Zhang reaction mechanisms will be analysed regarding their behaviour in the estimation of N_2O and we will shed light on the reasons behind their discrepancy at this condition.

Figures 11 and 12 show the most influential reactions on N_2O mole fractions with positive and the negative sensitivity coefficients estimated by Zhang and Klippenstein kinetic mechanisms, respectively. As can be seen in Fig. 11, reactions R1, H_2+O=H+OH (**R13**), H_2+OH=H+H_2O (**R14**) and 2OH=O+H_2O (**R15**) are the most important reactions that promote N_2O formation in the Klippenstein model, knowing that the previous reactions show no effect on N_2O mole fraction in Zhang mechanism. In addition, Zhang mechanism shows that NH+OH=HNO+H (**R16**), NH_2+O=HNO+H (**R17**), R2 and NH_2+H=NH+H_2 (**R18**) are the most dominant reactions boosting the mole fraction of N_2O by increasing the H and H_2 pools in the system, hence improving system's reactivity; it has been also noticed the ineffective action of these reactions in Klippenstein mechanism.

According to Fig. 12, both models show the highest negative sensitivity coefficient (Klippenstein: 17%, Zhang: 14%) for reaction R8, thus this reaction is considered the most influential in retarding N_2O formation. Along with that reactions N+NO=N_2+O (**R19**) and NH+NO=N_2+OH (**R20**) also show higher values in the Klippenstein model than the Zhang model. Several reactions have a high negative impact on the concentration of N_2O and their relative sensitivities are very similar in the two mechanisms, which was not the case for the N_2O formation promoting reactions. The variation in prediction of the sensitivity coefficient values is justified based on the differences in Arrhenius parameters of the two mechanisms.

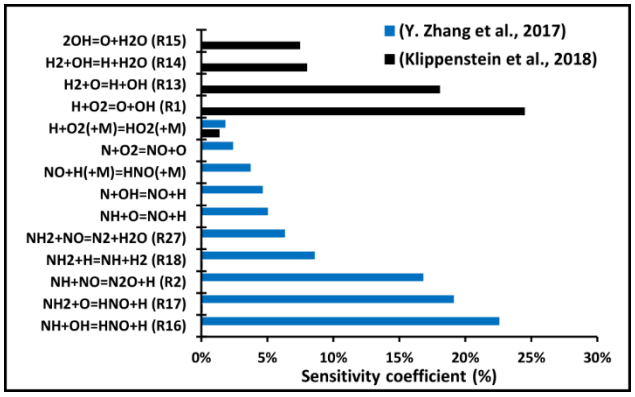

Fig.11. Reactions with the largest positive local sensitivity coefficients for N_2O mole fractions in 70/30 NH_3H_2 vol% premixed flame at φ=1 in the Klippenstein and Zhang kinetic models

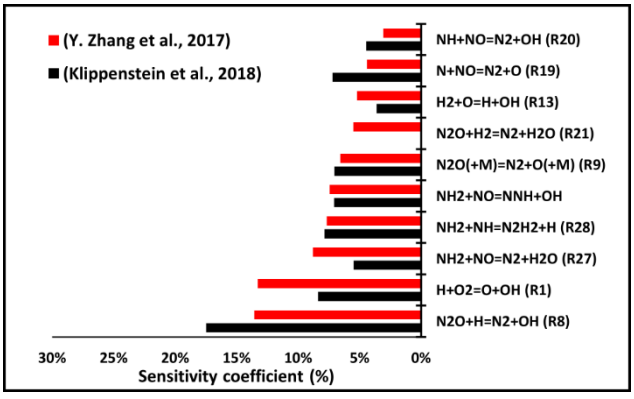

Fig. 12. Reactions with the largest negative local sensitivity coefficients for N_2O concentration in 70 NH_3/30 H_2 (%vol.) premixed flame at φ=1 in the Klippenstein and Zhang kinetic models

Figures 13 and 14 illustrate the rate distribution formation/consumption of N_2O along the computational domain estimated by Zhang and Klippenstein kinetic reaction mechanisms, respectively. As can be observed from the figures, the total component of N_2O increases at first, which is caused by the N_2O forming reaction R2. This phenomenon can be clearly observed for both selected kinetic models (see Fig. 15). Meanwhile, the consumption effect of reactions R8, $N_2O+H_2=N_2+H_2O$ (**R21**), R9, R12 and $NNH+O=N_2O+H$ (**R22**) is the reason behind the decline of the total N_2O (see Fig. 16).

It is also noticed that while in the Zhang mechanism reaction R21 is the second most influential in inhibiting N_2O formation, it is not even included in the Klippenstein mechanism. (see Fig. 16). Further, the N_2O production rates of reaction R2 estimated by Zhang mechanism is higher than that of Klippenstein. Similarly, the N_2O consumption rates of reactionsR9, R21 and R22 demonstrate higher consumption rates in the Zhang model than in the Klippenstein kinetic model.

Figure 17 illustrates the main pathways for the formation/ consumption of N_2O in terms of net reaction rate in the reaction zone where T=1619 K. As shown in the figure, formation of N_2O from NO occurs mainly (in 98%) via reaction with NH radicals according to R2, as well as dashed pathways: $NH_2+NO_2=N_2O+H_2O$ (**R23**) and

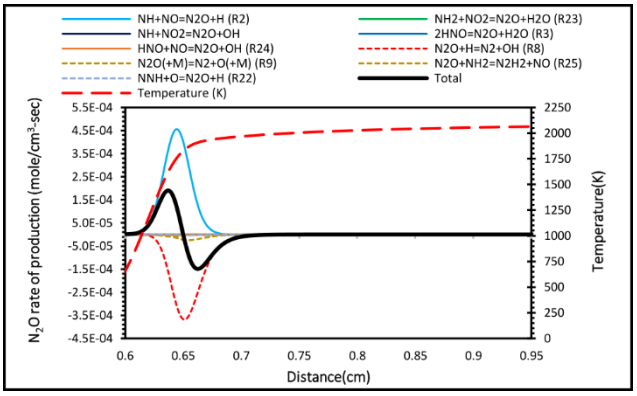

Fig. 13. The rate of production/consumption of N_2O in 70/30 vol% NH_3/H_2 mixture at stoichiometric conditions by model (Y. Zhang et al., 2017).

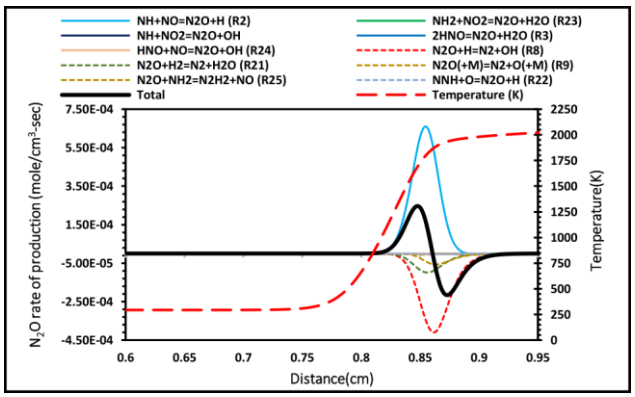

Fig. 14. The rate of production/consumption of N_2O in 70/30 vol% NH_3/H_2 mixture at stoichiometric conditions by model (Klippenstein et al., 2018).

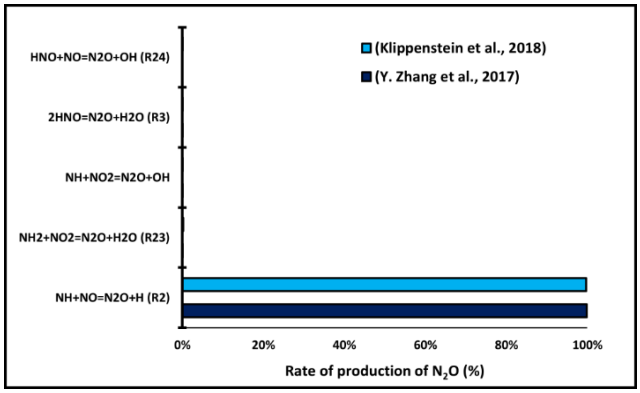

Fig. 15. Rate of production at stoichiometric conditions estimated by the (Y. Zhang et al., 2017) and (Klippenstein et al., 2018) kinetic models.

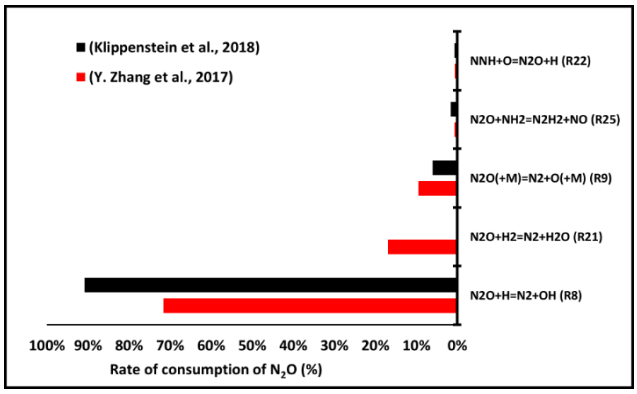

Fig.16. Rate of consumption at stoichiometric conditions estimated by the (Y. Zhang et al., 2017) and (Klippenstein et al., 2018). kinetic models.

$HNO+NO=N_2O+OH$ (**R24**) also contribute to the formation of N_2O. On the other hand, the chemical pathways for the consumption of N_2O shows that N_2O decomposes almost exclusively (in 99%) into N_2 by reacting with H atoms in reaction R8 (~0.97×99%=96%) and by unimolecular decay in R9 (~3%), whereas the remaining 1% of N_2O is consumed by reaction $N_2O+NH_2=N_2H_2+NO$ (**R25**).

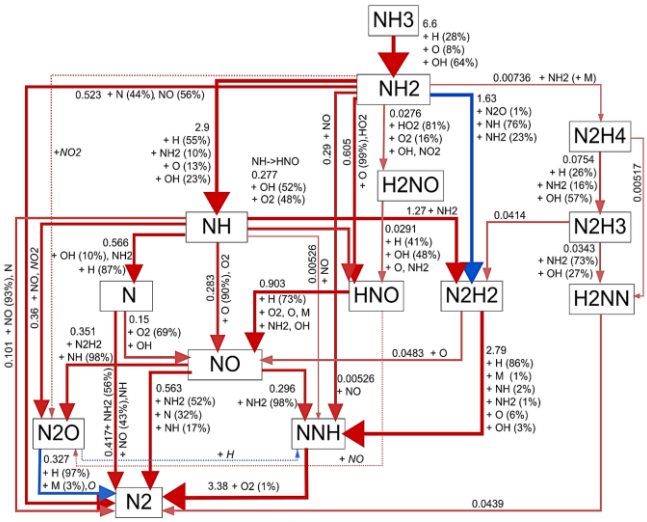

Fig. 17. Chemical reaction pathways of N_2O formation/consumption at flame zone (T=1619 K) and at φ=1 predicted by the Klippenstein model. Arrow lines refer to chemical transformations, percentages (%) refer to the contribution of reactants to the transformation, numbers stand for the net reaction rate in kmol/m^{3}s, which is also visualized by line

3.3 Rich flame conditions

The mole fraction of N_2O starts decreasing when the equivalence ratio increases to rich conditions and become close to zero at φ=1.4 (see Fig. 2). The performance of the tested mechanisms in predicting the mole fraction of N_2O deteriorate from φ=1.2, where many of the tested mechanisms give an estimated error over 20%. When φ increases to 1.4, the prediction accuracy of the kinetic mechanisms demonstrates a slight improvement (see Fig. 1). In addition, the prediction accuracy of the Klippenstein kinetic model has declined and the SMAPE has increased to 27%. Although the performance of Klippenstein kinetic mechanism at the rich conditions considerably deteriorates, several reaction mechanisms showed a superior performance in the estimation of N_2O. Such is the (Sun et al, 2022) kinetic model [41], which recorded 1% as SMAPE based on the experimental measurements. Therefore, both Klippenstein and Sun kinetic reaction mechanisms will be analysed in term of sensitivity and rate of formation/consumption of N_2O to examine the reasons behind their discrepancies at these conditions.

As shown in Figure 18, the N_2O mole fraction can be extremely boosted by the action of the reactions R2, $NH+H_2=NH_2+H$ (**R26**), $NH_2+NO=N_2+H_2O$ (**R27**) and R16. Reactions R2, R16 and R26 are responsible for increasing the system's reactivity by increasing the H pool. It should be highlighted that reaction R27 has no influence on N_2O mole fraction in the Klippenstein mechanism.

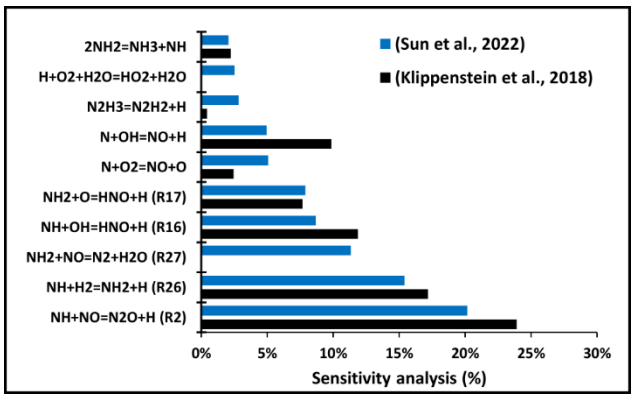

Fig. 18. Reactions with the largest positive local sensitivity coefficients for N_2O mole fraction in 70 NH_3/30 H_2 vol% premixed flame at φ=1.4 in the Klippenstein and Sun kinetic models

Figure 19 illustrates that reactions R1, R8, R27 and $N_2H_2+H=NH_2+NH$ (**R28**) has a considerable effect on reducing the concentration of N_2O by consuming H and NO species. Although both kinetic models show nearly the same reactions which have positive/negative trends on N_2O concentration, the estimated figures in most cases are different for the two mechanisms.

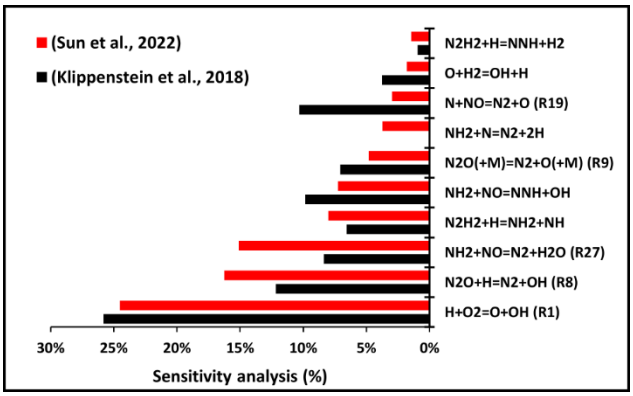

Fig. 19. Reactions with the largest negative local sensitivity coefficients for N_2O concentration in 70/30 vol% NH_3/H_2 premixed flame at φ=1.4 in the Klippenstein and Sun kinetic models.

As illustrated in Figs. 20 and 21, the increasing trend of the total N_2O can be explained by the increasing rate of the N_2O producing R2 reaction. Furthermore, both selected kinetic models give the same estimation for the N_2O production rate of reaction R2 (see Fig. 22). Meanwhile, the peaking rates of N_2O consuming reactions R8 and R9 cause the sharp decrease in the total rate of N_2O concentration change. In addition, the rate of reaction R8 estimated by the Klippenstein kinetic model is higher than that of Sun's reaction model (Fig. 23).

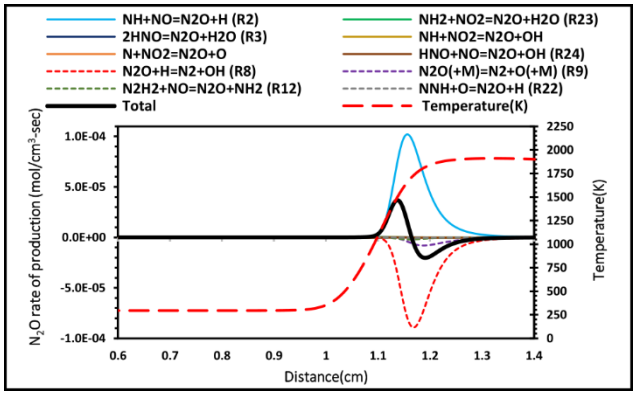

Fig. 20. The rate of production/consumption of N_2O in 70/30 vol% NH_3/H_2 mixture at φ=1.4 estimated by Sun kinetic model.

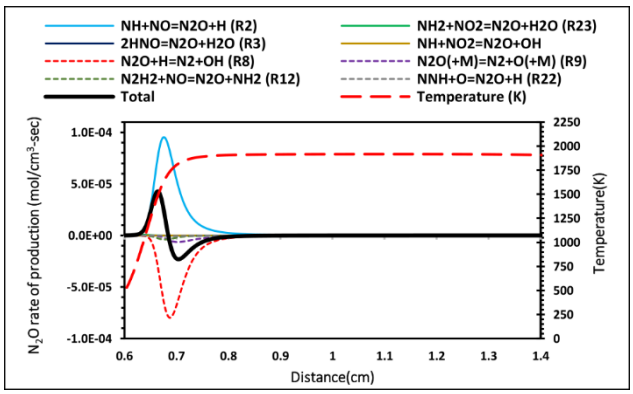

Fig. 21. The rate of production/consumption of N_2O in 70/30 vol% NH_3/H_2 mixture at φ=1.4 estimated by the Klippenstein kinetic models.

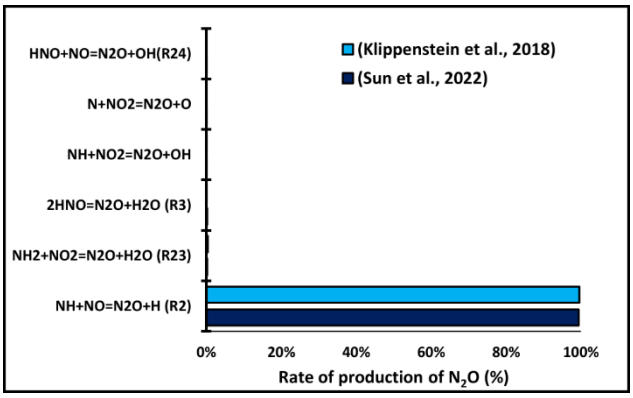

Fig. 22. Rate of production of N_2O at φ=1.4 estimated by the (Sun et al., 2022) and (Klippenstein et al., 2018) kinetic models.

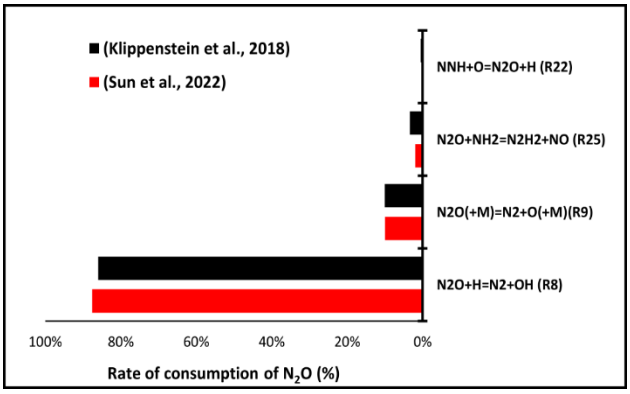

Fig. 23. Rate of consumption of N_2O at φ=1.4 estimated by the (Sun et al., 2022) and (Klippenstein et al., 2018) kinetic models.

It has been also observed the dominant role of the reaction R2 in increasing N_2O concentration, as well as the negative influence of reactions R8 and R9 on the consumption of N_2O at rich conditions can be seen clearly in the pathway diagram in Fig. 24.

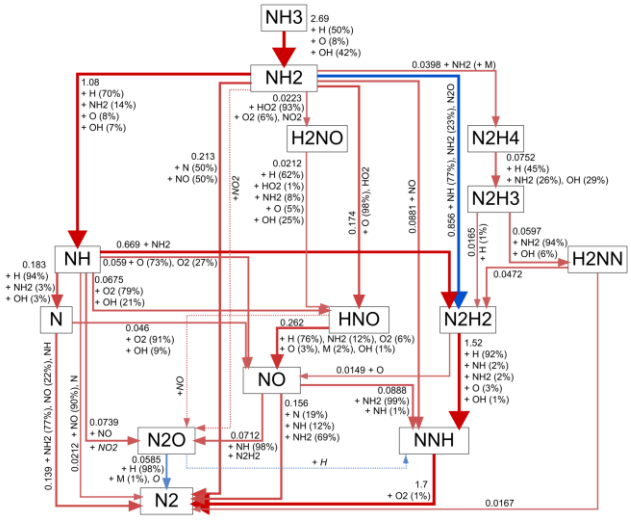

Fig. 24. Chemical reaction pathways of N_2O formation/consumption at flame zone (T= 1478K) and at φ=1.4 predicted by the Klippenstein kinetic model. Arrow lines refer to chemical transformations, percentages (%) refer to the contribution of reactants to the transformation, numbers stand for the net reaction rate in kmol/m^{3}s, which is also visualized by line thickness.

The diagram shows the rates at 1478K, which corresponds to the peak value of the total N_2O production rate. The pathway diagram shows that reaction NO+NH=N_2O+H (**R2**) accounts for about 98% of the NO to N_2O transformation. Further, reaction N_2O+H=N_2+OH (**R8**) is responsible in 98% for the decomposition of N_2O to N_2, and the formation of N_2H_2 from NH_2 takes place in 23% via reaction NH_2+N_2O=N_2H_2+NO (**R25**) (see blue lines in Fig. 24).

4. CONCLUSIONS

The present study numerically investigated the mole fraction of N_2O using 68 chemical kinetic mechanisms from the literature. The resulting numerical data was compared with experimental measurements from literature using symmetric mean absolute percentage error (SMAPE) to evaluate the performance of the selected mechanisms in predicting N_2O concentration in a 70/30 vol% NH_3/H_2 premixed flame. The study concludes that:

1. Most of the analysed chemical kinetic mechanisms exhibit low accuracy in predicting N_2O concentration at certain equivalence ratios, particularly very lean conditions (φ=0.6) and rich conditions (φ=1.2).
2. (Klippenstein et al, 2018) kinetic model generally predicts N_2O mole fractions accurately, but its performance deteriorates as the equivalence ratio increases from stoichiometric to rich conditions.
3. The chemical reaction NH+NO=N_2O+H plays a substantial part in the formation of N_2O for all tested conditions.
4. The consumption of N_2O is mainly governed by reactions N_2O+H=N_2+OH, N_2O(+M)=N_2+O(+M) and N_2O+NH_2=N_2H_2+NO, which show a domination role at all equivalence ratios.
5. For local conditions of φ, the (Nakamura et al, 2017) mechanism show good performance with 1% of error at 0.6, while the (Y. Zhang et al, 2017) and (Sun et al, 2022) kinetic models demonstrate proper performance at stoichiometry and rich conditions, with 3% and 1% errors, respectively.
6. The observed inconsistency among the reaction mechanisms in the estimation of N_2O mole fractions can be attributed to the variations in the reactions that control the consumption of N_2O. On the other hand, all the examined kinetic models showed analogous N_2O production rates and reactions governing N_2O generation.

5. ACKNOWLEDGMENTS

The authors gratefully acknowledge the support from EPSRC through the projects SAFE-AGT Pilot (no. EP/T009314/1) and Green Ammonia Thermal Propulsion MariNH3 (no. EP/W016656/1) as well as Joanna Jójka has received funding under a doctoral fellowship from the National Science Center, Poland, no. UMO-2019/32/T/ST8/00265. Furthermore, Ali Alnasif thanks Al-

Furat Al-Awsat Technical University (ATU) for the financial support of his PhD studies in the U.K. T. Nagy is grateful for the support of the FK134332 NKFIH grant.

5. REFERENCES

[1] IEA (2021), Global Energy Review 2021. Paris: International Energy Agency, Https://Www.Iea.Org/Reports/Global-Energy-Review-2021. (n.d.).

[2] G.R. Astbury, A review of the properties and hazards of some alternative fuels, Process Safety and Environmental Protection. 86 (2008) 397–414. https://doi.org/10.1016/J.PSEP.2008.05.001.

[3] A. Valera-Medina, H. Xiao, M. Owen-Jones, W.I.F. David, P.J. Bowen, Ammonia for power, Prog Energy Combust Sci. 69 (2018) 63–102. https://doi.org/10.1016/j.pecs.2018.07.001.

[4] W.S. Chai, Y. Bao, P. Jin, G. Tang, L. Zhou, A review on ammonia, ammonia-hydrogen and ammonia-methane fuels, Renewable and Sustainable Energy Reviews. 147 (2021). https://doi.org/10.1016/j.rser.2021.111254.

[5] P. Dimitriou, R. Javaid, A review of ammonia as a compression ignition engine fuel, Int J Hydrogen Energy. 45 (2020) 7098–7118. https://doi.org/10.1016/j.ijhydene.2019.12.209.

[6] A. Valera-Medina, F. Amer-Hatem, A.K. Azad, I.C. Dedoussi, M. de Joannon, R.X. Fernandes, P. Glarborg, H. Hashemi, X. He, S. Mashruk, J. McGowan, C. Mounaim-Rouselle, A. Ortiz-Prado, A. Ortiz-Valera, I. Rossetti, B. Shu, M. Yehia, H. Xiao, M. Costa, Review on ammonia as a potential fuel: From synthesis to economics, Energy and Fuels. 35 (2021) 6964–7029. https://doi.org/10.1021/acs.energyfuels.0c03685.

[7] P.J. Crutzen, H.G. Brauch, SPRINGER BRIEFS ON PIONEERS IN SCIENCE AND PRAC TICE NOBEL LAUREATES A Pioneer on Atmospheric Chemistry and Climate Change in the Anthropocene, n.d. http://www.afes-press-books.de/html/SpringerBriefs_PSP.htm.

[8] L.F. de Diego, C.A. Londonot, X.S. Wang, B.M. Gibbs, Influence of operating parameters on NOx and N20 axial profiles in a circulating fluidized bed combustor, 1996.

[9] A. Alnasif, S. Mashruk, M. Kovaleva, P. Wang, A. Valera-Medina, Experimental and numerical analyses of nitrogen oxides formation in a high ammonia-low hydrogen blend using a tangential swirl burner, Carbon Neutrality. 1 (2022). https://doi.org/10.1007/s43979-022-00021-9.

[10] A. Hayakawa, M. Hayashi, G.J. Gotama, M. Kovaleva, E.C. Okafor, S. Colson, T. Kudo, S. Mashruk, A. Valera-Medina, H. Kobayashi, N2O Production Characteristics of Ammonia/Hydrogen/Air Premixed Laminar Flames Stabilized in Stagnation Flows at Lean Conditions, 2021.

[11] S. Mashruk, E.C. Okafor, M. Kovaleva, A. Alnasif, D. Pugh, A. Hayakawa, A. Valera-Medina, Evolution of N2O production at lean combustion condition in NH3/H2/air premixed swirling flames, Combust Flame. 244 (2022) 112299. https://doi.org/10.1016/J.COMBUSTFLAME.2022.112299.

[12] G.J. Gotama, A. Hayakawa, E.C. Okafor, R. Kanoshima, M. Hayashi, T. Kudo, H. Kobayashi, Measurement of the laminar burning velocity and kinetics study of the importance of the hydrogen recovery mechanism of ammonia/hydrogen/air premixed flames, Combust Flame. 236 (2022). https://doi.org/10.1016/j.combustflame.2021.111753.

[13] H. Nakamura, S. Hasegawa, T. Tezuka, Kinetic modeling of ammonia/air weak flames in a micro flow reactor with a controlled temperature profile, Combust Flame. 185 (2017) 16–27. https://doi.org/10.1016/j.combustflame.2017.06.021.

[14] P. Glarborg, The NH3/NO2/O2 system: Constraining key steps in ammonia ignition and N2O formation, Combust Flame. (2022). https://doi.org/10.1016/j.combustflame.2022.112311.

[15] A. Stagni, C. Cavallotti, S. Arunthanayothin, Y. Song, O. Herbinet, F. Battin-Leclerc, T. Faravelli, An experimental, theoretical and kinetic-modeling study of the gas-phase oxidation of ammonia, React Chem Eng. 5 (2020) 696–711. https://doi.org/10.1039/c9re00429g.

[16] A. Bertolino, M. Fürst, A. Stagni, A. Frassoldati, M. Pelucchi, C. Cavallotti, T. Faravelli, A. Parente, An evolutionary, data-driven approach for mechanism optimization: theory and application to ammonia combustion, Combust Flame. 229 (2021). https://doi.org/10.1016/j.combustflame.2021.02.012.

[17] P. Dagaut, P. Glarborg, M.U. Alzueta, The oxidation of hydrogen cyanide and related chemistry, Prog Energy Combust Sci. 34 (2008) 1–46. https://doi.org/10.1016/j.pecs.2007.02.004.

[18] B. Mei, S. Ma, X. Zhang, Y. Li, Characterizing ammonia and nitric oxide interaction with outwardly propagating spherical flame method, Proceedings of the Combustion Institute. 38 (2021) 2477–2485. https://doi.org/10.1016/j.proci.2020.07.133.

[19] Gregory P. Smith, David M. Golden, Michael Frenklach, Nigel W. Moriarty, Boris Eiteneer, Mikhail Goldenberg, C. Thomas Bowman, Ronald K. Hanson, Soonho Song, William C. Gardiner, V.V.L. Jr., Zhiwei Qin, GRI-Mech 3.0, Http://Www.Me.Berkeley.Edu/Gri_mech/. (2000).

[20] X. Han, L.L. Marco, C. Brackmann, Z. Wang, Y. He, A.A. Konnov, Experimental and kinetic modeling study of NO formation in premixed CH4+O2+N2 flames, Combust Flame. 223 (2021) 349–360. https://doi.org/10.1016/j.combustflame.2020.10.010.

[21] E. Coda Zabetta, M. Hupa, A detailed kinetic mechanism including methanol and nitrogen pollutants relevant to the gas-phase combustion and pyrolysis of biomass-derived fuels, Combust Flame. 152 (2008) 14–27. https://doi.org/10.1016/j.combustflame.2007.06.022.

[22] B. Mei, J. Zhang, X. Shi, Z. Xi, Y. Li, Enhancement of ammonia combustion with partial fuel cracking strategy: Laminar flame propagation and kinetic modeling investigation of NH3/H2/N2/air mixtures up to 10 atm, Combust Flame. 231 (2021). https://doi.org/10.1016/j.combustflame.2021.111472.

[23] Alzueta MU, Zaragoza-2016 Mechanism , Personal Communication. (2016).

[24] A.G. Shmakov, O.P. Korobeinichev, I. v. Rybitskaya, A.A. Chernov, D.A. Knyazkov, T.A. Bolshova, A.A. Konnov, Formation and consumption of NO in H2 + O2 + N2 flames doped with NO or NH3 at atmospheric pressure, Combust Flame. 157 (2010) 556–565. https://doi.org/10.1016/j.combustflame.2009.10.008.

[25] K.P. Shrestha, C. Lhuillier, A.A. Barbosa, P. Brequigny, F. Contino, C. Mounaïm-Rousselle, L. Seidel, F. Mauss, An experimental and modeling study of ammonia with enriched oxygen content and ammonia/hydrogen laminar flame speed at elevated pressure and temperature, Proceedings of the Combustion Institute. 38 (2021) 2163–2174. https://doi.org/10.1016/j.proci.2020.06.197.

[26] C. Esarte, M. Peg, M.P. Ruiz, Á. Millera, R. Bilbao, M.U. Alzueta, Pyrolysis of ethanol: Gas and soot products formed, Ind Eng Chem Res. 50 (2011) 4412–4419. https://doi.org/10.1021/ie1022628.

[27] Z. Wang, X. Han, Y. He, R. Zhu, Y. Zhu, Z. Zhou, K. Cen, Experimental and kinetic study on the laminar burning velocities of NH3 mixing with CH3OH and C2H5OH in premixed flames, Combust Flame. 229 (2021). https://doi.org/10.1016/j.combustflame.2021.02.038.

[28] M. Abian, M.U. Alzueta, P. Glarborg, Formation of NO from N2/O2 mixtures in a flow reactor: Toward an accurate prediction of thermal NO, Int J Chem Kinet. 47 (2015) 518–532. https://doi.org/10.1002/kin.20929.

[29] X. Zhang, S.P. Moosakutty, R.P. Rajan, M. Younes, S.M. Sarathy, Combustion chemistry of ammonia/hydrogen mixtures: Jet-stirred reactor measurements and comprehensive kinetic modeling, Combust Flame. 234 (2021). https://doi.org/10.1016/j.combustflame.2021.111653.

[30] T. Wang, X. Zhang, J. Zhang, X. Hou, Automatic generation of a kinetic skeletal mechanism for methane-hydrogen blends with nitrogen chemistry, Int J Hydrogen Energy. 43 (2018) 3330–3341. https://doi.org/10.1016/j.ijhydene.2017.12.116.

[31] S. Arunthanayothin, A. Stagni, Y. Song, O. Herbinet, T. Faravelli, F. Battin-Leclerc, Ammonia-methane interaction in jet-stirred and flow reactors: An experimental and kinetic modeling study, in: Proceedings of the Combustion Institute, Elsevier Ltd, 2021: pp. 345–353. https://doi.org/10.1016/j.proci.2020.07.061.

[32] T. Faravelli, POLIMI-2017, Personal Communication. (2017).

[33] POLIMI, The CRECK Modeling Group,C1-C3 mechanism , Http://Creckmodeling.Chem.Polimi.It. (2014).

[34] X. Han, Z. Wang, M. Costa, Z. Sun, Y. He, K. Cen, Experimental and kinetic modeling study of laminar burning velocities of NH3/air, NH3/H2/air, NH3/CO/air and NH3/CH4/air premixed flames, Combust Flame. 206 (2019) 214–226. https://doi.org/10.1016/j.combustflame.2019.05.003.

[35] C.S.T. Marques, L.R. dos Santos, M.E. Sbampato, L.G. Barreta, A.M. dos Santos, TEMPERATURE MEASUREMENTS BY OH

LIF AND CHEMILUMINESCENCE KINETIC MODELING FOR ETHANOL FLAMES, 2073.
[36] S. de Persis, L. Pillier, M. Idir, J. Molet, N. Lamoureux, P. Desgroux, NO formation in high pressure premixed flames: Experimental results and validation of a new revised reaction mechanism, Fuel. 260 (2020). https://doi.org/10.1016/j.fuel.2019.116331.
[37] V. Aranda, J.M. Christensen, M.U. Alzueta, P. Glarborg, S. Gersen, Y. Gao, P. Marshall, Experimental and kinetic modeling study of methanol ignition and oxidation at high pressure, Int J Chem Kinet. 45 (2013) 283–294. https://doi.org/10.1002/kin.20764.
[38] B. Mei, X. Zhang, S. Ma, M. Cui, H. Guo, Z. Cao, Y. Li, Experimental and kinetic modeling investigation on the laminar flame propagation of ammonia under oxygen enrichment and elevated pressure conditions, Combust Flame. 210 (2019) 236–246. https://doi.org/10.1016/j.combustflame.2019.08.033.
[39] Y. Jiang, A. Gruber, K. Seshadri, F. Williams, An updated short chemical-kinetic nitrogen mechanism for carbon-free combustion applications, Int J Energy Res. 44 (2020) 795–810. https://doi.org/10.1002/er.4891.
[40] R. Li, A.A. Konnov, G. He, F. Qin, D. Zhang, Chemical mechanism development and reduction for combustion of NH3/H2/CH4 mixtures, Fuel. 257 (2019). https://doi.org/10.1016/j.fuel.2019.116059.
[41] J. Sun, Q. Yang, N. Zhao, M. Chen, H. Zheng, Numerically study of CH4/NH3 combustion characteristics in an industrial gas turbine combustor based on a reduced mechanism, Fuel. 327 (2022) 124897. https://doi.org/10.1016/J.FUEL.2022.124897.
[42] E.C. Okafor, Y. Naito, S. Colson, A. Ichikawa, T. Kudo, A. Hayakawa, H. Kobayashi, Measurement and modelling of the laminar burning velocity of methane-ammonia-air flames at high pressures using a reduced reaction mechanism, Combust Flame. 204 (2019) 162–175. https://doi.org/10.1016/j.combustflame.2019.03.008.
[43] Y. Song, L. Marrodán, N. Vin, O. Herbinet, E. Assaf, C. Fittschen, A. Stagni, T. Faravelli, M.U. Alzueta, F. Battin-Leclerc, The sensitizing effects of NO 2 and NO on methane low temperature oxidation in a jet stirred reactor, Proceedings of the Combustion Institute. 37 (2019) 667–675. https://doi.org/10.1016/j.proci.2018.06.115.
[44] P. Glarborg, J.A. Miller, B. Ruscic, S.J. Klippenstein, Modeling nitrogen chemistry in combustion, Prog Energy Combust Sci. 67 (2018) 31–68. https://doi.org/10.1016/j.pecs.2018.01.002.
[45] R. Mével, S. Javoy, F. Lafosse, N. Chaumeix, G. Dupré, C.E. Paillard, Hydrogen–nitrous oxide delay times: Shock tube experimental study and kinetic modelling, Proceedings of the Combustion Institute. 32 (2009) 359–366. https://doi.org/10.1016/J.PROCI.2008.06.171.
[46] K.P. Shrestha, L. Seidel, T. Zeuch, F. Mauss, Detailed Kinetic Mechanism for the Oxidation of Ammonia Including the Formation and Reduction of Nitrogen Oxides, Energy and Fuels. 32 (2018) 10202–10217. https://doi.org/10.1021/acs.energyfuels.8b01056.
[47] R.C. da Rocha, M. Costa, X.S. Bai, Chemical kinetic modelling of ammonia/hydrogen/air ignition, premixed flame propagation and NO emission, Fuel. 246 (2019) 24–33. https://doi.org/10.1016/J.FUEL.2019.02.102.
[48] J. Otomo, M. Koshi, T. Mitsumori, H. Iwasaki, K. Yamada, Chemical kinetic modeling of ammonia oxidation with improved reaction mechanism for ammonia/air and ammonia/hydrogen/air combustion, Int J Hydrogen Energy. 43 (2018) 3004–3014. https://doi.org/10.1016/j.ijhydene.2017.12.066.
[49] U. Mechanism, Chemical-kinetic mechanisms for combustion applications, Mechanical and Aerospace Engineering (Combustion Research), University of California at San Diego. (2018).
[50] S.J. Klippenstein, M. Pfeifle, A.W. Jasper, P. Glarborg, Theory and modeling of relevance to prompt-NO formation at high pressure, Combust Flame. 195 (2018) 3–17. https://doi.org/10.1016/j.combustflame.2018.04.029.
[51] M. Kovaleva, A. Hayakawa, S. Colson, E.C. Okafor, T. Kudo, A. Valera-Medina, H. Kobayashi, Numerical and experimental study of product gas characteristics in premixed ammonia/methane/air laminar flames stabilised in a stagnation flow, Fuel Communications. 10 (2022) 100054. https://doi.org/10.1016/j.jfueco.2022.100054.
[52] E. Houshfar, Ø. Skreiberg, P. Glarborg, T. Løvas, Reduced chemical kinetic mechanisms for NO x emission prediction in biomass combustion, Int J Chem Kinet. 44 (2012) 219–231. https://doi.org/10.1002/kin.20716.
[53] Y. Zhang, O. Mathieu, E.L. Petersen, G. Bourque, H.J. Curran, Assessing the predictions of a NOx kinetic mechanism on recent hydrogen and syngas experimental data, Combust Flame. 182 (2017) 122–141. https://doi.org/10.1016/j.combustflame.2017.03.019.
[54] N. Lamoureux, H. el Merhubi, L. Pillier, S. de Persis, P. Desgroux, Modeling of NO formation in low pressure premixed flames, Combust Flame. 163 (2016) 557–575. https://doi.org/10.1016/j.combustflame.2015.11.007.
[55] H. Xiao, A. Valera-Medina, P.J. Bowen, Modeling Combustion of Ammonia/Hydrogen Fuel Blends under Gas Turbine Conditions, Energy and Fuels. 31 (2017) 8631–8642. https://doi.org/10.1021/acs.energyfuels.7b00709.
[56] G. Capriolo, C. Brackmann, M. Lubrano Lavadera, T. Methling, A.A. Konnov, An experimental and kinetic modeling study on nitric oxide formation in premixed C3alcohols flames, in: Proceedings of the Combustion Institute, Elsevier Ltd, 2021: pp. 805–812. https://doi.org/10.1016/j.proci.2020.07.051.
[57] Y. Song, H. Hashemi, J.M. Christensen, C. Zou, P. Marshall, P. Glarborg, Ammonia oxidation at high pressure and intermediate temperatures, Fuel. 181 (2016) 358–365. https://doi.org/10.1016/j.fuel.2016.04.100.
[58] L. Xu, Y. Chang, M. Treacy, Y. Zhou, M. Jia, X.S. Bai, A skeletal chemical kinetic mechanism for ammonia/n-heptane combustion, Fuel. 331 (2023). https://doi.org/10.1016/j.fuel.2022.125830.
[59] H. Nozari, A. Karabeyoılu, Numerical study of combustion characteristics of ammonia as a renewable fuel and establishment of reduced reaction mechanisms, Fuel. 159 (2015) 223–233. https://doi.org/10.1016/j.fuel.2015.06.075.
[60] D.E. Thomas, K.P. Shrestha, F. Mauss, W.F. Northrop, ARTICLE IN PRESS Extinction and NO formation of ammonia-hydrogen and air non-premixed counterflow flames, Proceedings of the Combustion Institute. (2022). https://doi.org/10.1016/j.proci.2022.08.067.
[61] O. Mathieu, E.L. Petersen, Experimental and modeling study on the high-temperature oxidation of Ammonia and related NOx chemistry, Combust Flame. 162 (2015) 554–570. https://doi.org/10.1016/j.combustflame.2014.08.022.
[62] M. Kovács, M. Papp, I.G. Zsély, T. Turányi, Determination of rate parameters of key N/H/O elementary reactions based on H2/O2/NOx combustion experiments, Fuel. 264 (2020) 116720. https://doi.org/10.1016/J.FUEL.2019.116720.
[63] C. Duynslaegher, F. Contino, J. Vandooren, H. Jeanmart, Modeling of ammonia combustion at low pressure, Combust Flame. 159 (2012) 2799–2805. https://doi.org/10.1016/j.combustflame.2012.06.003.
[64] M. Kovács Máté Papp István Gy Zsély Tamás Turányi, Main sources of uncertainty in recent methanol/NOx combustion models, Int J Chem Kinet. 53 (2021) 884–900. https://doi.org/10.1002/kin.21490.
[65] S.J. Klippenstein, L.B. Harding, P. Glarborg, J.A. Miller, The role of NNH in NO formation and control, Combust Flame. 158 (2011) 774–789. https://doi.org/10.1016/j.combustflame.2010.12.013.
[66] M. Kovács, M. Papp, I.G. Zsély, T. Turányi, Determination of rate parameters of key N/H/O elementary reactions based on H2/O2/NOx combustion experiments, Fuel. 264 (2020) 116720. https://doi.org/10.1016/J.FUEL.2019.116720.
[67] K. Zhang, Y. Li, T. Yuan, J. Cai, P. Glarborg, F. Qi, An experimental and kinetic modeling study of premixed nitromethane flames at low pressure, Proceedings of the Combustion Institute. 33 (2011) 407–414. https://doi.org/10.1016/j.proci.2010.06.002.
[68] P. Saxena, F.A. Williams, Numerical and experimental studies of ethanol flames, Proceedings of the Combustion Institute. 31 I (2007) 1149–1156. https://doi.org/10.1016/j.proci.2006.08.097.
[69] N. Lamoureux, P. Desgroux, A. el Bakali, J.F. Pauwels, Experimental and numerical study of the role of NCN in prompt-NO formation in low-pressure CH4-O2-N2 and C2H2-O2-N2 flames, Combust Flame. 157 (2010) 1929–1941. https://doi.org/10.1016/j.combustflame.2010.03.013.
[70] É. Valkó, M. Papp, M. Kovács, T. Varga, I. Gy Zsély, T. Nagy, T. Turányi, Combustion Theory and Modelling ISSN: (Print) (Design of combustion experiments using differential entropy Design of combustion experiments using differential entropy, Combustion Theory and Modelling. 26 (2022) 67–90.

https://doi.org/10.1080/13647830.2021.1992506.
[71] A.A. Konnov, Implementation of the NCN pathway of prompt-NO formation in the detailed reaction mechanism, Combust Flame. 156 (2009) 2093–2105. https://doi.org/10.1016/j.combustflame.2009.03.016.
[72] M.U. Alzueta, R. Bilbao, M. Finestra, Methanol oxidation and its interaction with nitric oxide, Energy and Fuels. 15 (2001) 724–729. https://doi.org/10.1021/ef0002602.
[73] T. Mendiara, P. Glarborg, Ammonia chemistry in oxy-fuel combustion of methane, Combust Flame. 156 (2009) 1937–1949. https://doi.org/10.1016/j.combustflame.2009.07.006.
[74] H. Nakamura, M. Shindo, Effects of radiation heat loss on laminar premixed ammonia/air flames, Proceedings of the Combustion Institute. 37 (2019) 1741–1748. https://doi.org/10.1016/j.proci.2018.06.138.
[75] Z. Tian, Y. Li, L. Zhang, P. Glarborg, F. Qi, An experimental and kinetic modeling study of premixed NH3/CH4/O2/Ar flames at low pressure, Combust Flame. 156 (2009) 1413–1426. https://doi.org/10.1016/j.combustflame.2009.03.005.
[76] A. Hayakawa, M. Hayashi, M. Kovaleva, G.J. Gotama, E.C. Okafor, S. Colson, S. Mashruk, A. Valera-Medina, T. Kudo, H. Kobayashi, Experimental and numerical study of product gas and N2O emission characteristics of ammonia/hydrogen/air premixed laminar flames stabilized in a stagnation flow, Proceedings of the Combustion Institute. (2022). https://doi.org/10.1016/j.proci.2022.08.124.
[77] J.S. Armstrong, F. Collopy, Error measures for generalizing about forecasting methods: Empirical comparisons *, 1992.